Available online at www.sciencedirect.com

ScienceDirect

IFAC PapersOnline CONFERENCE PAPER ARCHIVE

IFAC PapersOnLine 55-30 (2022) 254–259

Nonlinear and divergent responses of fluctuation-driven systems

Moritz Thümler * **Malte Schröder.** ** **Marc Timme** ***

* *Center for Advancing Electronics Dresden (cfaed) and Institute for Theoretical Physics, Technische Universität Dresden, 01062 Dresden, Germany (e-mail: moritz.thuemler@tu-dresden.de).*

** *Center for Advancing Electronics Dresden (cfaed) and Institute for Theoretical Physics, 01062 Technische Universität Dresden, Dresden, Germany (e-mail: malte.schroeder@tu-dresden.de)*

*** *Center for Advancing Electronics Dresden (cfaed); Institute for Theoretical Physics, Technische Universität Dresden, and Cluster of Excellence Physics of Life, Technische Universität Dresden, 01062 Dresden, Germany; Lakeside Labs, 9020 Klagenfurt am Wörthersee, Austria (e-mail: marc.timme@tu-dresden.de)*

Abstract: Most network dynamical systems are out of equilibrium and externally driven by fluctuations. Linear response theory generically characterizes systems responses to such fluctuations for small driving amplitudes yet cannot capture response properties that are either due to strong driving or intrinsically nonlinear. For oscillation-driven systems, we here report average response offsets that scale quadratically with asymptotically small amplitudes. At some critical driving amplitude, responses cease to stay close to a given operating point and may diverge. Standard response theory fails to predict these amplitudes even at arbitrarily high orders. We propose an integral self-consistency condition that captures the full nonlinear system dynamics. We illustrate our approach for a minimal one-dimensional model and capture the nonlinear shift of voltages in the phase, frequency and voltage dynamics of AC power grid networks. Our approach may help to quantitatively predict intrinsically nonlinear response dynamics as well as bifurcations emerging at large driving amplitudes in non-autonomous dynamical systems.

Keywords: Nonautonomous systems, nonlinear response functions, fluctuations, nonlocal prediction, linear response theory, power grids

1. INTRODUCTION

Networked systems abound. Their dynamics and reliable function fundamentally underlies our daily lives, from the networks of neurons in the brain that make us think to metabolic networks that fuel our cells and from water supply networks to electric power grids. All of these systems are out of equilibrium and driven by external inputs or fluctuations. Yet, most standard literature on dynamical systems' theory focuses on autonomous systems that are not externally driven.

A key overarching question is how strongly systems that reside at given operating points in the absence of driving respond to a driving signal of given strength. From the perspective of dynamical systems theory, this translates to the question of how systems initialized sufficiently close to a stable fixed point, periodic orbit, or other stable invariant set, respond dynamically if driven by a signal of some strength ε. Specifically, linear response theory [Bender et al. 1999, Strogatz 2018, Zhang et al. 2019] provides a general method to predict deviations $\Delta x(t)$ away from a fixed point $x^* \in \mathbb{R}^N$ in response to sufficiently weak driving signals, $\varepsilon g(t)$ where ε is small. However, stronger, temporally correlated driving signals impinging on nonlinear systems may cause nonlinear, nonlocal and so far unpredictable responses.

Here we focus on a basic class of problems where a nonlinear system initially near a stable fixed point (or periodic orbit) is driven by strong periodic signals. Despite the naive intuition that for symmetric sinusoidal driving the response should be zero on average, we observe that average responses are generically nonlinearly offset from the original fixed points. Moreover, if the signal amplitude grows too large, $\varepsilon > \varepsilon_{\mathrm{crit}}$, the response may diverge and never return anywhere close to the original fixed point. Such nonlocal bifurcations emerging at large $\varepsilon_{\mathrm{crit}}$ are impossible to predict via standard series expansions, even at arbitrarily high order because polynomials in ε of any order are finite at all $\varepsilon \in \mathbb{R}$. Extending linear (first order) response theory, we propose an integral method of approximation that exploits a self-consistency condition of

⋆ Bundesministerium für Bildung und Forschung (BMBF) under grant No. 03EK3055F; Deutsche Forschungsgemeinschaft (DFG, German Research Foundation) under Germanys Excellence Strategy – EXC-2068 – 390729961– Cluster of Excellence Physics of Life of TU Dresden

10.1016/j.ifacol.2022.11.061

average zero shift of the fluctuating part of the response. The method demonstrates that local response solution ceases to exist at some finite $\varepsilon_{\text{crit}}$ and enables to explicitly approximate that value. The proposed integral method thus yields a qualitative and reasonable quantitative prediction of the point at which responses start to diverge. We illustrate our findings for a simple one-dimensional model.

2. DYNAMICAL SYSTEMS SETTING

Let us consider network dynamical systems consisting of N units with time evolution given via coupled nonlinear ordinary differential equations

$$\frac{\mathrm{d}\boldsymbol{x}}{\mathrm{d}t} = \boldsymbol{f}(\boldsymbol{x}) + \varepsilon \boldsymbol{g}(t) \tag{1}$$

with the dynamical variables $\boldsymbol{x}(t) \in \mathbb{R}^N$, a smooth nonlinear function $f : \mathbb{R}^N \to \mathbb{R}^N$ and external time-dependent fluctuations $g : \mathbb{R} \to \mathbb{R}^N$ with zero long term average. The strength is tuned by a positive scalar parameter $\varepsilon \in \mathbb{R}_0^+$. We further consider that the system has an operating point as given by a stable fixed point $\boldsymbol{x}^* \in \mathbb{R}^N$ of the undriven dynamical system at $\varepsilon = 0$, hence implicitly determined by

$$0 = \boldsymbol{f}(\boldsymbol{x}^*). \tag{2}$$

If the autonomous systems' Jacobian $J = \mathrm{D}\boldsymbol{f}|_{\boldsymbol{x}^*} \in \mathbb{R}^{N\times N}$ with matrix elements

$$J_{nm} = \frac{\partial f_n}{\partial x_m}(\boldsymbol{x}^*), \tag{3}$$

is negative definite, i.e., all eigenvalues λ of J have a negative real part $\mathrm{Re}(\lambda) < 0$, an open neighborhood of $\mathcal{U}(\boldsymbol{x}^*) \subset \mathbb{R}^N$ of $\boldsymbol{x}^*$ exists such that trajectories started at initial conditions $\boldsymbol{x}(0) \in \mathcal{U}(\boldsymbol{x}^*)$ evolve towards the fixed point $\boldsymbol{x}^*$ [Strogatz 2018] for $\varepsilon = 0$. We explore the response dynamics of networked systems and here consider two main questions. First, how does the response dynamics of the system change with ε? Second, can we identify a critical fluctuation strength $\varepsilon_{\text{crit}}$ above which the systems' response leaves the neighborhood $\mathcal{U}(\boldsymbol{x}^*)$? While standard (linear-) response theory [Bender et al. 1999, Zhang et al. 2019] provides insights about the first question under standard conditions and asymptotically for $\varepsilon \to 0$, the second question is generally hard to answer.

In this article, we restrict ourselves to the simplest of such fluctuations, periodic and in particular sinusoidal fluctuations acting on only one dynamical variable k such that

$$g_n(t) = \delta_{n,k} \cos(\omega_0 t), \tag{4}$$

with the Kronecker symbol $\delta_{n,k}$ equal to one for $n = k$ and zero otherwise. Moreover, we set the initial condition $x(t = 0) = x^*$ in all calculations.

This article is structured as follows: we first introduce a motivating example, a model of power grid dynamics including voltage dynamics, for which we illustrate the core dynamical effects of interest to us, the scaling of the average nonlinear offset with ε and the boundary of existence of stationary response. Second, we explicate these phenomena in a one-dimensional simple model, for which we develop analytic methods to quantify scaling and critical $\varepsilon_{\text{crit}}$ beyond which stationary responses break down. Finally, we apply the developed methods to the one-dimensional and the original power grid model.

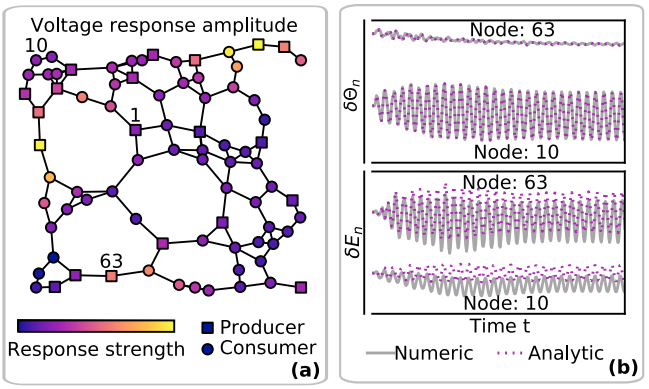

Fig. 1. **Dynamic responses in a power grid model. (a)** Model network indicating distributed amplitudes of voltage responses δE (bottom) across network. Marked node 1 is driven by a sinusoidal fluctuation $\varepsilon \sin(t)$. **(b)** Response dynamics at nodes $i \in \{10, 63\}$ to driving node $k = 1$. Analytically determined linear response (purple) and actual (numerically integrated) system dynamics (gray). After a transient, the voltage responses δE_i exhibit a constant average operating offset not predicted by linear response theory, most clearly visible for node 10. (Parameters: $B_{nm} = 4$ if a connection between node n and m exists, $B_{nn} = -\sum_m B_{nm}$ and $B_{nm} = 0$ otherwise, $P_n = 3$ for producers and $P_n = -1$ for consumers, $X_n = 1.0$, $E^f = 3$, $\alpha = 0.02$, and $\omega^{(0)} = 2\pi$.

3. FLUCTUATION-DRIVEN DYNAMICS OF A POWER GRID MODEL.

Most aspects of our daily life essentially depend on a reliable supply of electrical power, thereby imposing severe challenges for stable operation of power grids that consist of many generators (producers of electric power) and loads (consumers of power) connected with transmission lines. From a perspective of network dynamical systems [Witthaut et al. 2022], these challenges translate to requiring steady states that are (asymptotically) stable against sufficiently small fluctuations. As a consequence, all dynamical variables relax back to their steady synchronous (phase-locked) state. Let us first evaluate the dynamics of the third order model of power grids that describes N synchronous machines interconnected with alternating current (AC) transmission lines [Machowski et al. 2011, Schmietendorf et al. 2014]. Each synchronous machine state is described by three dynamical variables: a rotor angle $\Theta_n(t) \in \mathbb{R}$, the rotor frequency $\omega_n(t) \in \mathbb{R}$, and a voltage amplitude $E_n(t) \in \mathbb{R}_0^+$. The rotor frequency ω_n is proportional to deviations from the nominal grid frequency, i.e. 50 Hz in Europe [Owen 1997], which together with the voltage amplitudes are crucial to power system stability [Machowski et al. 2011]. The model [Machowski et al. 2011, Schmietendorf et al. 2014, Thümler et al. 2022] is given by

$$\dot{\Theta}_n = \omega_n$$
$$\dot{\omega}_n = P_n - \alpha\omega_n + \sum_{m=1}^{N} B_{nm}E_nE_m \sin(\Theta_m - \Theta_n) + \delta_{nk}\varepsilon g_n(t)$$
$$\dot{E}_n = E^f - E_n + X_n \sum_{m=1}^{N} B_{nm}E_m \cos(\Theta_m - \Theta_n), \quad (5)$$

where $B \in \mathbb{R}^{N\times N}$, is the symmetric susceptance matrix encoding the topology of the power grid and P_n the active power inserted ($P_n > 0$) or taken out ($P_n < 0$) by the machine n. Moreover, E^f, X_n, $\alpha \in \mathbb{R}_0^+$ denote positive system parameters. The frequency of node k is perturbed periodically with frequency $\omega^{(0)}$ and amplitude $\varepsilon \geq 0$. Here, we consider the system close to a stable fixed point $(\boldsymbol{\Theta}^*, \boldsymbol{\omega}^*, \boldsymbol{E}^*) \in \mathbb{R}^{3N}$, as defined in Eq. 2 which represents a phase-locked state of fixed phase differences and thus fixed power transmission. As an example, the dynamics of such a system with $N = 80$ nodes is displayed in Fig. 1 when perturbed at the node $k = 1$. The Figure illustrates patterns of response amplitudes across the network (panel a), explained previously by [Zhang et al. 2019] for the second order model ($X_n = 0$ such that $E_n(t) = E^f$ for all $n \in \{1, 2, ..., N\}$), and an additional nonlinear operating offset $\overline{E}_n$ in the voltages (panel b) that are present in the voltage variables E_n if the system is perturbed periodically. Numerically, the operating offset is determined according to

$$\overline{\boldsymbol{E}} = \frac{1}{\Delta t}\int_{t_1}^{t_1+\Delta t} \boldsymbol{E}(t)\,\mathrm{d}t - \boldsymbol{E}^*, \quad (6)$$

for $\Delta t \gg T_\omega =: 2\pi/\omega^{(0)}$ and sufficiently large t_1 to ensure that transient dynamics have declined. In practice, the trajectory $\boldsymbol{E}(t)$ is obtained by numerical integration of system (5). In Fig. 1 this offset $\overline{\boldsymbol{E}}$ is visible when comparing the linear response with the numerically integrated response dynamics for the voltage variables. In Fig. 3 the operating offsets $\overline{\boldsymbol{E}}$ are displayed against the perturbation strength ε. We observe that the scaling of the operating offset is proportional to ε^2 asymptotically as $\varepsilon \to 0$, showing that this operating offset is an inherently nonlinear effect. Moreover, solutions near the original fixed point cease to exist for $\varepsilon > \varepsilon_{\text{crit}} \approx 2.4$. Here $\overline{\boldsymbol{E}}$ is still well-defined but $\overline{\boldsymbol{E}} + \boldsymbol{E}^*$ lies outside the neighborhood $\mathcal{U}(\boldsymbol{\Theta}^*, \boldsymbol{\omega}^*, \boldsymbol{E}^*)$. Such a solution is known as a low voltage solution, obtained after a voltage drop of the power system, an undesired operational state usually causing power outages [Machowski et al. 2011]. To understand the origin of the nonlinearity and the ceasing of solutions in the original stability neighborhood, let us study a simpler model.

4. ONE-DIMENSIONAL MODEL AND METHODS

To explicitly capture the nonlinear operating offset and its breakdown analytically, we study a one-dimensional model given by

$$\frac{dx}{dt} = f(x) + \varepsilon\cos(\omega t) := \alpha - \cos(x) + \varepsilon\cos(\omega t), \quad (7)$$

with $x \in \mathbb{R}$ and a model parameter $\alpha \in [0, 1]$. The linearly stable fixed points x^* for $\varepsilon = 0$ are given by

$$x^* = 2\pi\ell - \arccos(\alpha), \quad (8)$$

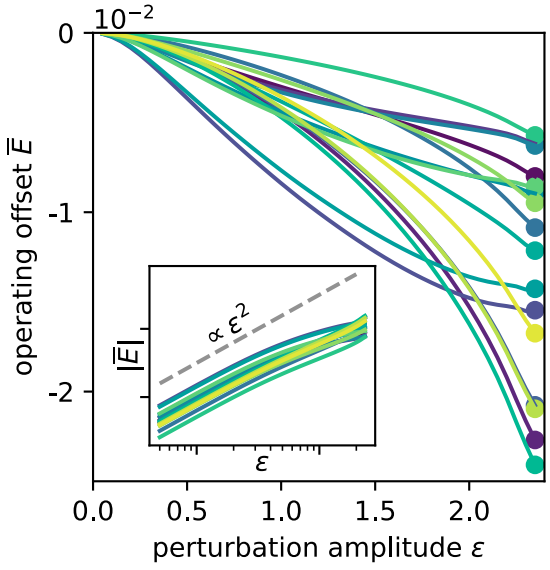

Fig. 2. **Nonlinear operating offset of the voltage response scales with ε^2.** The voltage operating offsets $\overline{E}_n$ as a function of the perturbation amplitude ε for 16 randomly drawn nodes n of the network in Fig. 1. Inset: Absolute values $|\delta E|$ plotted double logarithmically indicates nonlinear scaling for small ε. At some large $\varepsilon_{\text{crit}}$ the trajectories leave the stable neighborhood $\mathcal{U}(\boldsymbol{\Theta}^*, \boldsymbol{\omega}^*, \boldsymbol{E}^*)$ and the description of the operating offset breaks down.

with $\ell \in \mathbb{Z}$. Hence, the parameter α is defining the location of the fixed points x^* and the slope and curvature of the function $f(x)$ at x^*. For clarity, we pick the one fixed point for $\ell = 0$. Like in the power grid model, the one dimensional model Eq. (7) shows an operating offset $\overline{x}$ when exposed to periodic signals. If the perturbation strength increases beyond a critical perturbation strength $\epsilon_{\text{crit}} \approx 7$ for the example shown in Fig. 3, the response dynamics diverge to $+\infty$ for $t \to \infty$. Numerically, the operating offset $\overline{x}$ is measured in the same way as in Eq. (6) and scales quadratic with ϵ for, $\epsilon \to 0$, as shown in Fig. 3c.

4.1 Response theory in ε

Let us first recapitulate dynamical response theory up to second order for the one-dimensional model defined by Eq. (7). We write the response dynamics $x(t)$ as a formal power series [Bender et al. 1999] in ε such that

$$x(t) = \sum_{n=0}^{\infty} a_n(t)\varepsilon^n \sim x^* + a_1(t)\varepsilon + a_2(t)\varepsilon^2 \text{ as } \varepsilon \to 0, \quad (9)$$

with functions $a_n : \mathbb{R} \to \mathbb{R}$. The aim of perturbation theory is to find the functions $a_n(t)$ up to a desired order M, proceeding as follows. Expanding the nonlinear function $f(x)$ into a Taylor series about the fixed point x^* up to ε^M and substituting the power series (9) into the differential equation (7) yields

$$\varepsilon\dot{a}_1 + \varepsilon^2\dot{a}_2 \sim f(x^*) + \varepsilon\cos(\omega t) + f'(x^*)\left(\varepsilon a_1 + \varepsilon^2 a_2\right) + \frac{1}{2}f''(x^*)\varepsilon^2 a_1^2 \text{ as } \varepsilon \to 0, \quad (10)$$

where $\dot{a}_n$ refers to the first derivative of a_n with respect to t and $f'(x)$ and $f''(x)$ refer to first and second derivatives of $f(x)$ with respect to x. If the power series (10) is

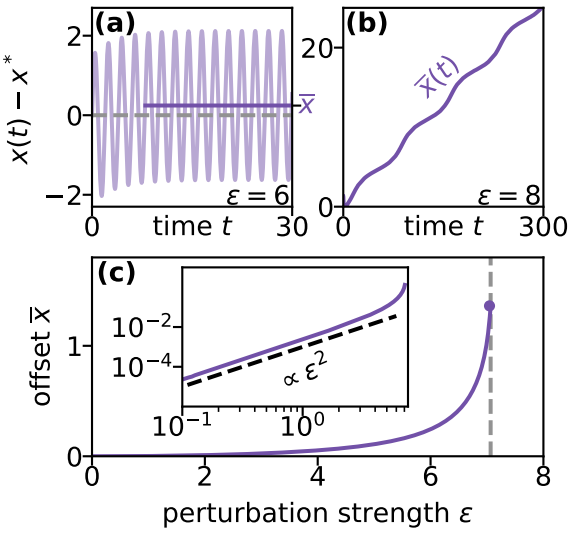

Fig. 3. **Nonlinear operating offset and response diverergence in simple model**. Response dynamics as a function of driving amplitude for the one-dimensional model (7). **(a)** Response dynamics relative to the fixed point x^* as a function of time for moderate driving amplitude $\varepsilon = 6$. Offset $\overline{x}$ determined in analogy to Eq. (6) marked at right vertical axis. **(b)** For larger $\varepsilon = 8$, an estimate $\overline{x}(t)$ (with $\Delta t = 2$) continually increases with time and no steady solution is assumed. **(c)** Nonlinear quadratic scaling of the operating offset $\overline{x}$ asymptotically as $\varepsilon \to 0$, the same as for the power system model, see Fig. 3. Parameters: $\alpha = 0.1$, $\omega = \pi$.

convergent, the coefficients of powers of ε are unique, such that we can equate coefficients for identical powers of ε to obtain

$$\boxed{\varepsilon^1:} \quad \dot{a}_1(t) = f'(x^*)a_1(t) + \cos(\omega t)$$
$$\boxed{\varepsilon^2:} \quad \dot{a}_2(t) = f'(x^*)a_2(t) + \frac{1}{2}f''(x^*)a_1^2(t)\,. \qquad (11)$$

To solve for $a_n(t)$, one starts with $n = 1$ and iteratively solves the linear inhomogeneous differential equations for $a_{n+1}(t)$ given in terms of the inhomogeneities $a_n(t)$ (and the driving term for $n = 1$). For our example system, the function $a_1(t)$ – the linear response function – is given by (see Eq. (A.8) derived in the appendix)

$$a_1(t) = |A_1|\cos(\omega t + \arg(A_1)) - \mathrm{Re}(A_1)e^{f'(x^*)t}, \qquad (12)$$

with the response factor

$$A_1 = \frac{1}{\imath\omega - f'(x^*)} \in \mathbb{C}. \qquad (13)$$

The initial condition $x(0) = x^*$ implies $a_n(0) = 0$ for all $n \in \mathbb{N}$. The linear response function $a_1(t)$ has a transient term, declining over time as $f'(x^*) < 0$ and a part that is fluctuating symmetrically around the fixed point x^*, as expected, providing no information about the operating offset $\overline{x}$ whatsoever.

4.2 Nonlinear offset from second order response theory

We aim at determining the average (and thus temporally constant) nonlinear operating offset $\overline{x}$ around which the response dynamics $x(t)$ fluctuate in the long term, i.e., after some transient. The linear response function, $a_1(t)$ Eq. (12), cannot help us in this matter, as it is composed of time-varying terms only. However, the second order response function $a_2(t)$ exhibits an offset. We determine the constant part without solving for the time variation of the function $a_2(t)$ as follows. First, consider

$$a_1(t) \sim |A_1|\cos(\omega t) \text{ as } t \to \infty, \qquad (14)$$

because $f'(x^*) < 0$, and neglecting the phase $\arg(A_1)$, such that

$$\dot{a}_2(t) \sim f'(x^*)a_2(t) + \frac{f''(x^*)|A_1|^2}{4}(\cos(2\omega t) + 1), \qquad (15)$$

where we applied the trigonometric identity $\cos^2(x) = (\cos(2x) + 1)/2$. Utilizing the superposition principle for linear equations, we compute a fixed point of Eq. (15) neglecting the $\cos(\cdot)$ term, yielding

$$\overline{a}_2 = -\frac{|A_1|^2 f''(x^*)}{4f'(x^*)}, \qquad (16)$$

as a first approximation of the nonlinear operating offset $\overline{x}$, this is sufficient as Eq. (15) has the same form as the differential equation for $a_1(t)$ for which fluctuating perturbations cannot contribute to an offset. From Eq. (15) we learn that the offset

$$\overline{x}(\varepsilon) \sim \overline{a}_2\varepsilon^2 =: \overline{x}^{\mathrm{S}} \text{ as } \varepsilon \to 0 \qquad (17)$$

scales quadratically in the lowest order of amplitude ε of the driving signal, just as for the power grid example above, see Fig. 3. Moreover, the nonlinear magnitude of the offset increases with the curvature of $f(x)$ at x^*. The superscript "^{S}" marks an approximation obtained via standard second order response theory. It is contrasted with an alternative integral method we propose below for estimating the same quantity.

4.3 Nonlocal response theory to predict divergence – the integral method

Second order response theory correctly predicts the nonlinear (quadratic) scaling of the response offset, yet it cannot tell us at which driving amplitude ε_c such periodic responses cease to exist and even whether they ever stop existing. Furthermore, any polynomial approximation necessarily fails because polynomial functions always evaluate to some finite number given an argument. Standard second and higher order perturbation theory thus fails to inform us about diverging response amplitudes. We now introduce an alternative method of approximating the response, exploiting an incompleteness that arises in an integral consistency condition if a first order response approximation is evaluated instead of the exact periodic response. We require that response trajectories are periodic with the same periodicity $T_\omega = 2\pi/\omega$ as the perturbation. Integrating the nonlinear differential equation Eq. (7) on both sides over one period T_ω then cancels all periodic terms, especially the perturbation term, and yields

$$0 = \frac{1}{T_\omega}\int_{t_1}^{t_1+T_\omega} \dot{x}(t)\,\mathrm{d}t = \frac{1}{T_\omega}\int_{t_1}^{t_1+T_\omega} f(x(t))\,\mathrm{d}t. \qquad (18)$$

However, as we do not know the true solution $x(t)$ to our problem, but rather just an approximation for small ε such as in Eq. (10), we cannot expect that the right-hand side

of Eq. (18) is identically zero if we replace $x(t)$ with its linear response $x^* + \varepsilon a_1(t)$ approximation. We exploit this discrepancy by demanding that

$$0 = \lim_{t_1 \to \infty} \frac{1}{T_\omega} \int_{t_1}^{t_1+T_\omega} f(x^* + \varepsilon a_1(t) + \overline{x}^I(\varepsilon))\, \mathrm{d}t \qquad (19)$$

holds for a newly and implicitly defined function $\overline{x}^I(\varepsilon)$ that we consider as an alternative, higher order approximation for the actual nonlinear operating offset $\overline{x}(\varepsilon)$. Depending on the explicit model nonlinearity $f(x)$, the integral Eq. (19) may or may not be analytically solvable.

4.4 Prediction of response divergence

For the one-dimensional example model (7), the method is analytically executable to yield an implicit equation directly for an approximation $\varepsilon^I_{\mathrm{crit}}$ for the critical driving amplitude $\varepsilon_{\mathrm{crit}}$ (and not only for $\overline{x}^I(\varepsilon)$).

We apply both response theoretic approaches, the standard second order response theory and the integral method, to that model (7). First, relations (16) and (17) explicitly yield

$$\overline{x}^S = \varepsilon^2 \frac{\cos(x^*)}{4(\omega^2 + \sin^2(x^*))\sin(x^*)}, \qquad (20)$$

yielding an offset for all $\varepsilon \in \mathbb{R}$. As discussed above, as a simple polynomial in ε, this second order estimate clearly fails to predict that or for which $\varepsilon_{\mathrm{crit}}$ local response solutions cease to exist and responses start to diverge.

In contrast, the integral approach expresses $\overline{x}^I$ as a function of ε and $\varepsilon_{\mathrm{crit}}$ as follows. Due to the periodicity condition, we have

$$\begin{aligned} 0 &= \lim_{t_1 \to \infty} \frac{1}{T_\omega} \int_{t_1}^{t_1+T_\omega} f(x^* + a_1(t)\varepsilon + \overline{x}^I(\varepsilon))\, \mathrm{d}t \\ &= \frac{1}{T_\omega} \int_0^{T_\omega} \left[\alpha - \cos(x^* + \varepsilon|A_1|\cos(\omega t) + \overline{x}^I)\right]\, \mathrm{d}t \\ &= \alpha - \cos(x^* + \overline{x}^I) \frac{1}{T_\omega} \int_0^{T_\omega} \cos(\varepsilon|A_1|\cos(\omega t))\, \mathrm{d}t \\ &= \alpha - \cos(x^* - \overline{x}^I) J_0(\varepsilon|A_1|), \end{aligned} \qquad (21)$$

in terms of the Bessel function of the first kind $J_0(z) = \pi^{-1} \int_0^\pi \cos(z\sin(\tau))\, \mathrm{d}\tau$. The offset predicted by the integral method thus is

$$\bar{x}^I(\varepsilon) = \arccos\left[\frac{\alpha}{J_0(\varepsilon|A_1|)}\right] - x^*. \qquad (22)$$

In contrast to the standard second order approximation (20) for the average offset, the integral approximation (22) has bounded support in ε due to the limited domain $(-1, 1)$ of the $\arccos(\cdot)$ function. It is thus capable of predicting that divergent responses emerge and approximately at which $\varepsilon_{\mathrm{crit}}$ they diverge and leave the neighborhood $\mathcal{U}(x^*)$ of the fixed point. We exploit this feature to extract $\varepsilon^I_{\mathrm{crit}}$ from the condition of maximal support

$$\varepsilon^I_{\mathrm{crit}} = \frac{J_0^{-1}(\alpha)}{|A_1|}, \qquad (23)$$

with a local inverse J_0^{-1} of the Bessel function, an answer to the second question we raised in the introduction.

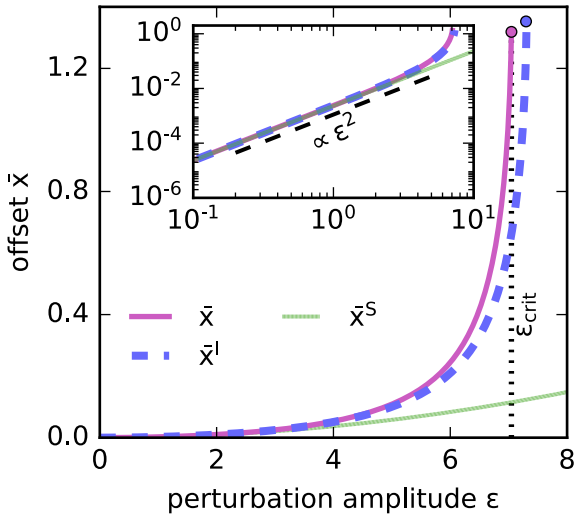

Fig. 4. **Integral method predicts offset and critical $\varepsilon_{\mathrm{crit}}$** The approximation $\bar{x}^I(\varepsilon)$ (dashed blue, Eq. (22)) matches the nonlinear offset (purple) in model (7) and well predicts the critical perturbation amplitude $\varepsilon_{\mathrm{crit}}$ (vertical dotted line where the purple curve ends) above which no steady response exists. Integral method provides prediction $\bar{x}^I$ as the upper limit where Eq. (22) does not have a real solution. Second order response theory estimate $\bar{x}^S(\varepsilon)$ (green) becomes highly inaccurate at higher perturbation amplitudes and does not capture the breakdown of the steady response. (inset) For small ε all approximations agree and asymptotically scale as $\bar{x} \propto \varepsilon^2$. The parameters are the same as in Fig. 3.

Figure 4 shows a comparison of the actual $\overline{x}(\varepsilon)$ with its approximations $\overline{x}^S(\varepsilon)$ and $\overline{x}^I(\varepsilon)$. For $\varepsilon \to 0$ all curves agree and scale $\propto \varepsilon^2$. For larger ε the approximation $\overline{x}^I(\varepsilon)$ obtained from the integral method still well resembles the actual value $\overline{x}(\varepsilon)$ yet its second order standard prediction $\overline{x}^S(\varepsilon)$ disagrees strongly. For ε of the order of $\varepsilon_{\mathrm{crit}}$, $\overline{x}^I(\varepsilon)$ still resembles the actual value and $\varepsilon^I_{\mathrm{crit}}$ accurately predicts the point of failure. The standard second order estimator does not indicate any $\varepsilon_{\mathrm{crit}}$ due to its polynomial nature.

5. CONCLUSION

In summary, we have reported a nonlinear operating offset $\overline{x}$ and the ultimate loss of local reponses for flucutation-driven systems. The offset characterizes a non-zero average of a temporally fluctuating response near an operating point determined by an undriven system, i.e., a fixed point $\boldsymbol{x}^*$. It scales with the square of the perturbation strength, ε^2 asymptotically as $\varepsilon \to 0$. Linear response theory generically does not capture such offsets at all. We have demonstrated that standard second order response theory predicts an offset $\overline{x}^S$ that captures the asymptotic scaling as $\varepsilon \to 0$ but necessarily fails to predict the existence (and position) of a critical driving strength $\varepsilon_{\mathrm{crit}}$ (small or large) above which response trajectories diverge from a local neighborhood $\mathcal{U}(\boldsymbol{x}^*)$.

We have introduced an alternative approach that is jointly capable of both, approximating the nonlinear scaling and

predicting critical driving strengths. It is based on a consistency condition of integral form and has qualitatively new features compared to standard nonlinear response theory. First, it is capable of expanding the range of validity beyond small ε. Second, it provides a condition for the value $\varepsilon_{\mathrm{crit}}$ even if that is large and as such captures non-local influences. We have explicated one model applications where the estimator is computable analytically. Specifically, all (linear response, standard second order response and non-standard integral) approaches have been tested on a simple, one-dimensional model. Our estimator correctly captures the nonlinear scaling, as well as the fact that local solutions fail to exist beyond some critical driving strength. For the one-dimensional model, the estimator is quantitatively accurate. Possible improvements for larger systems include utilizing higher order response theories within the integral approach.

The nonlocal integral method relies on the stationary dynamics, i.e., post transient dynamics only. Therefore, transient dynamics causing the system to leave the neighborhood $\mathcal{U}(x^*)$ cannot be captured by this method. It is conceivable that the integral method might be extendable to capture also basic trends set by transient dynamics, e.g. exponential decays or linear drifts.

In addition, several research directions open up. The example of the one-dimensional system has illustrated how increasing driving amplitudes cause the system to permanently leave a local neighborhood set by an unstable fixed point closest to the operating point x^*, marking the boundary of the basin of attraction of x^*. It remains unclear how the method transfers to more complex basin boundaries. More generally, which types of loss of local responses, and tipping points caused by the driving, can be identified with the integral method? A thorough investigation of systems near known bifurcations may be valuable to fill in these knowledge gaps. Identifying suitable approximations for the extracting explicit approximate expressions for $\varepsilon_{\mathrm{crit}}$ would therefore be desirable.

REFERENCES

Bender, C.M., Orszag, S., and Orszag, S.A. (1999). *Advanced mathematical methods for scientists and engineers I: Asymptotic methods and perturbation theory*, volume 1. Springer Science & Business Media.

Machowski, J., Bialek, J., and Bumby, J. (2011). *Power System Dynamics: Stability and Control*. Wiley. URL https://books.google.de/books?id=wZv92UdKxi4C.

Owen, E. (1997). The origins of 60-Hz as a power frequency. *IEEE Industry Applications Magazine*, 3(6), 8–14. doi:10.1109/2943.628099. URL https://doi.org/10.1109/2943.628099.

Schmietendorf, K., Peinke, J., Friedrich, R., and Kamps, O. (2014). Self-organized synchronization and voltage stability in networks of synchronous machines. *The European Physical Journal Special Topics*, 223(12), 2577–2592. doi:10.1140/epjst/e2014-02209-8. URL https://doi.org/10.1140/epjst/e2014-02209-8.

Strogatz, S.H. (2018). *Nonlinear Dynamics and Chaos*. CRC Press. doi:10.1201/9780429492563. URL https://doi.org/10.1201/9780429492563.

Thümler, M., Zhang, X., and Timme, M. (2022). Absence of pure voltage instabilities in the third-order model of power grid dynamics. *Chaos: An Interdisciplinary Journal of Nonlinear Science*, 32(4), 043105. doi:10.1063/5.0080284. URL https://doi.org/10.1063/5.0080284.

Witthaut, D., Hellmann, F., Kurths, J., Kettemann, S., Meyer-Ortmanns, H., and Timme, M. (2022). Collective nonlinear dynamics and self-organization in decentralized power grids. *Reviews of Modern Physics*, 94(1). doi:10.1103/revmodphys.94.015005. URL https://doi.org/10.1103/revmodphys.94.015005.

Zhang, X., Hallerberg, S., Matthiae, M., Witthaut, D., and Timme, M. (2019). Fluctuation-induced distributed resonances in oscillatory networks. *Science Advances*, 5(7), eaav1027. doi:10.1126/sciadv.aav1027. URL https://doi.org/10.1126/sciadv.aav1027.

Appendix A. METHODS

A.1 Response theory in one dimensional systems

Here, we present a known derivation of the linear response function $a_1(t)$, defined via the differential equation

$$\dot{a}_1(t) = f'(x^*)a_1(t) + \cos(\omega t), \tag{A.1}$$

with the initial condition $a_1(0) = 0$. For this purpose, it is useful to make an excursion to the complex plane and solve the following differential equation for $y(t)$

$$\dot{y}(t) = f'(x^*)y(t) + e^{\imath\omega t}, \tag{A.2}$$

and afterwards obtaining $a_1(t) = \mathrm{Re}(y(t))$. The homogeneous solution $y_{\mathrm{h}}(t)$ of the separable, linear differential equation is given by

$$y_{\mathrm{h}}(t) = Ce^{f'(x^*)t}. \tag{A.3}$$

A particular solution is obtained by the method of variations of the constant, which we explicate in the following. We take the homogeneous solution and treat the constant C as being time dependent itself $C \to C_p(t)$ and inserting this function on both sides of the differential equation

$$\begin{aligned} \dot{C}_p(t) \quad & e^{f'(x^*)t} + C_p(t)f'(x^*)e^{f'(x^*)t} \\ = \quad & C_p(t)f'(x)e^{f'(x^*)t} + e^{\imath\omega t} \\ \Rightarrow C_p(t) &= \frac{1}{\imath\omega - f'(x^*)}e^{\imath\omega t - f'(x^*)t} \ . \end{aligned} \tag{A.4}$$

The particular solution follows as

$$y_{\mathrm{p}}(t) = C_p(t)e^{f'(x^*)t} = \frac{1}{\imath\omega - f'(x^*)}e^{\imath\omega t}. \tag{A.5}$$

The comprehensive set of solutions of the linear differential equation is then given by the superposition of homogenous and particular solution

$$y(t) = y_{\mathrm{h}}(t) + y_{\mathrm{p}}(t) = Ce^{f'(x^*)t} + \frac{1}{\imath\omega - f'(x^*)}e^{\imath\omega t}, \tag{A.6}$$

where the constant of integration C can be determined from the initial condition $y(0) = a_1(0) = 0$, yielding

$$y(t) = \frac{1}{\imath\omega - f'(x^*)}\left(e^{\imath\omega t} - e^{f'(x^*)}\right) =: A_1\left(e^{\imath\omega t} - e^{f'(x^*)t}\right). \tag{A.7}$$

We obtain $a_1(t)$ as the real part of $y(t)$

$$\begin{aligned} a_1(t) &= \mathrm{Re}\left(A_1e^{i\omega t} - A_1e^{f'(x^*)t}\right) \\ &= |A_1|\cos(\omega t + \arg(A_1)) - \mathrm{Re}(A_1)e^{f'(x^*)t}, \end{aligned} \tag{A.8}$$

which is the solution we referenced in the main text.